

Anomalous temperature dependence of the electrical resistivity in binary and pseudobinary alloys based on Fe₃Si

Yoichi Nishino, Shin-ya Inoue, and Shigeru Asano

Department of Materials Science and Engineering, Nagoya Institute of Technology, Showa-ku, Nagoya 466, Japan

Nobuo Kawamiya

Chukyo University, Showa-ku, Nagoya 466, Japan

(Received 2 July 1993)

The electrical resistivity of binary Fe-Si and ternary (Fe_{1-x}M_x)₃Si alloys, with 3d transition-metal elements $M = \text{Ti, V, Cr, Mn, Co, and Ni}$, has been measured over the temperature range from 4.2 to 1373 K. The resistivity for $M = \text{Ti, V, Cr, and Mn}$ shows an anomalous temperature dependence: an occurrence of a resistance maximum near the Curie point T_C and a negative resistivity slope above T_C . The tendency of the negative temperature dependence of the resistivity increases markedly with increasing composition, accompanying a sharp reduction in T_C . In contrast, the resistivity curves for $M = \text{Co and Ni}$ exhibit almost the same form as that of Fe₃Si, regardless of the Co or Ni composition, so that the resistivity above T_C remains almost constant or decreases slightly. The negative temperature dependence induced by M substitution appears only when the resistivity estimated in the paramagnetic state is above 150 $\mu\Omega$ cm, and the higher paramagnetic resistivity causes the lower temperature coefficient of the resistivity. It is concluded that the resistance maximum in (Fe_{1-x}M_x)₃Si is closely related to an extremely large spin-disorder scattering, in addition to a high residual resistivity.

I. INTRODUCTION

The intermetallic compound Fe₃Si is a well-ordered ferromagnet with a $D0_3$ crystal structure. This structure has two inequivalent sites for Fe atoms with specific neighbor configurations, which are named an Fe_I and an Fe_{II} site. The former has eight Fe nearest neighbors, while the latter has four Fe and four Si nearest neighbors. A characteristic property of Fe₃Si is that transition-metal impurities substitute for the Fe_I or the Fe_{II} site selectively, as proved in nuclear magnetic resonance studies¹ and subsequently confirmed by neutron diffraction,² Mössbauer spectroscopy,³ and x-ray absorption studies.⁴

Niculescu, Burch, and Budnick⁵ have extensively investigated the site preference of substituting 3d transition atoms in Fe₃Si. Thus in the (Fe_{1-x}M_x)₃Si system,^{5,6} the elements to the left of Fe in the periodic table, i.e., $M = \text{Ti, V, Cr, and Mn}$, show a strong preference for the Fe_I site, whereas those to the right, such as $M = \text{Co and Ni}$, occupy the Fe_{II} site. The occurrence of the selective site substitution has also been supported by energy-band calculations,⁷⁻⁹ which predict that the site preference is correlated with the partial density of states for each Fe site in Fe₃Si and thus enhances the lattice cohesion for the pseudobinary system.

The selective site substitution of 3d transition-metal impurities has further been demonstrated for (Fe_{1-x}M_x)₃Ga,^{10,11} where the $D0_3$ phase is always stabilized, although Fe₃Ga forms an $L1_2$ phase in the equilibrium state, unlike Fe₃Si and Fe₃Al. Especially for (Fe_{1-x}V_x)₃Ga and (Fe_{1-x}Ti_x)₃Ga, we have recently found an anomalous temperature dependence of the electrical resistivity,^{11,12} characterized by a resistance maximum near the Curie point T_C and a negative resistivity slope at the higher temperatures up to 1000 K and above.

This negative temperature dependence above T_C is the most striking feature, which has been first observed in ferromagnetic 3d alloys. It has been suggested that (Fe_{1-x}M_x)₃Ga is a new type of conductor not to be classified into several other types of metallic conductors hitherto known to exhibit a negative temperature coefficient of resistivity.¹²

The anomalous resistance behavior described above is expected to take place in a series of $D0_3$ -type Fe₃D ($D = \text{Ga, Si, Al, etc.}$) ferromagnetic alloys in which Fe atoms are partly replaced by the other 3d transition atoms. In the present study, we have employed Fe₃Si as a base material and systematically investigated the temperature dependence of the electrical resistivity in the pseudobinary alloys (Fe_{1-x}M_x)₃Si with $M = \text{Ti, V, Cr, Mn, Co, and Ni}$. The purpose of this study is to clarify which 3d transition-metal impurities are liable for the occurrence of the negative temperature dependence of the resistivity, and to examine the electrical resistance maximum near T_C in regard to the anomaly in the magnetic scattering resistivity.

II. EXPERIMENT

A. Sample preparation

The Fe-Si binary alloys and the (Fe_{1-x}M_x)₃Si pseudobinary alloys were made from 99.99% pure Fe and Si, and $M = \text{Ti, V, Cr, Mn, Co, and Ni}$ of at least 99.9% purity. Appropriately composed mixtures of the constituents were melted in an argon arc furnace, followed by

several remeltings to achieve homogeneity. The weight loss during the melting procedure was less than 0.5%, and the nominal composition assigned to each sample was regarded as accurate. The ingots were heat-treated at 1123 K for 144 ks in vacuum to form an ordered structure. Samples for the resistivity measurements were cut from the ingots with an alumina-blade saw to the size of $1 \times 1 \times 20 \text{ mm}^3$. Each sample, sealed in an evacuated quartz capsule, was annealed at 773 K for 3.6 ks and furnace-cooled to room temperature.

B. X-ray analysis

X-ray diffraction was measured with Cu $K\alpha$ radiation on powder samples prepared as above. Figure 1 shows the lattice parameters of the DO_3 phase in $(\text{Fe}_{1-x}\text{M}_x)_3\text{Si}$ as a function of composition x for $M = \text{Ti, V, Cr, Mn, Co, and Ni}$. A single phase of the DO_3 structure was formed in the composition range shown by the solid lines, whereas a small amount of additional phase was also detected in the range shown by the dotted lines, where the (111) and (200) superlattice reflections were reduced in intensity. These results are consistent with those previously reported by Niculescu and Budnick.¹³

In the case of $M = \text{Co}$, the lattice parameter decreases with composition x , maintaining the single-phase state up to $x = 0.6$. This means that the lattice contraction occurred presumably because of enhanced cohesion by the DO_3 -type ordering. On the contrary, the lattice dilatation for $M = \text{Ti, V, Cr, Mn, and Ni}$ is much smaller than that estimated from each Fe- M primary (bcc) solid solutions.¹⁴ Hence, the substitution of all the $3d$ metals is considered to contract the lattice spacings as a result of the stabilization of the DO_3 phase.

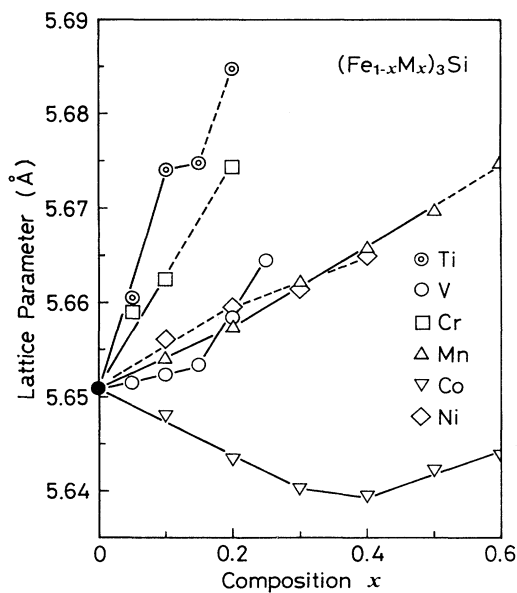


FIG. 1. Lattice parameters of the DO_3 phase in $(\text{Fe}_{1-x}\text{M}_x)_3\text{Si}$ as a function of composition x for $M = \text{Ti, V, Cr, Mn, Co, and Ni}$. The DO_3 single-phase state is obtained in the range represented by the solid lines.

C. Measurements

The electrical resistivity was measured by a standard dc four-terminal method with a current of 100 mA over the temperature range from 4.2 to 1373 K and with a rising rate of 0.03 K/s. The measurements at high temperatures were carried out in vacuum of 3×10^{-4} Pa. The Curie temperature T_C was determined by means of differential thermal analysis.

III. EXPERIMENTAL RESULTS

A. Fe-Si binary system

The electrical resistivity was measured as a function of temperature for pure Fe and Fe-Si alloys containing 7–40 at. % Si as shown in Fig. 2: each curve is shifted along the ordinate. In these alloys, an inflection of the curves was found around the Curie temperatures T_C indicated by the arrows. The resistivity of Fe-7 at. % Si exhibits a sharp variation below T_C and a linear dependence with a positive slope of $0.02 \mu\Omega \text{ cm/K}$ above T_C . When the DO_3 phase is formed, however, the resistivity above T_C remains almost constant for Fe-15 and -20 at. % Si but gradually decreases with rising temperature for Fe-25 and -30 at. % Si. The decrease in the resistivity is associated with the formation of the DO_3 -type Fe_3Si since the curve of Fe-40 at. % Si shows a normal temperature dependence. A similar type of resistance anomaly has also been reported for Fe-Pd alloys,^{15,16} which has been explained by the formation of $L1_2$ -type long-range order for FePd_3 below the order-disorder transition temperature.

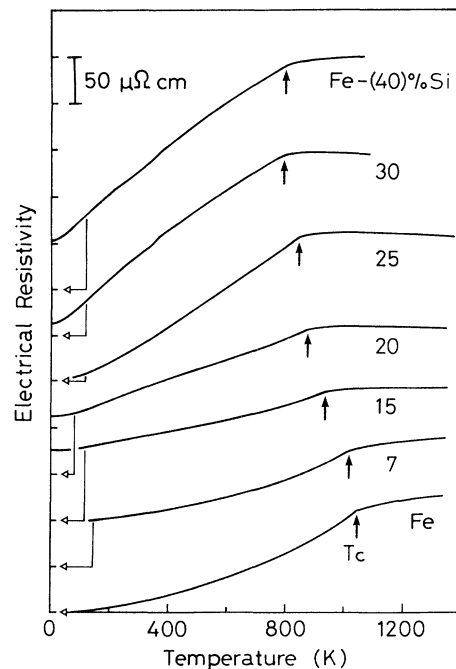


FIG. 2. Temperature dependence of electrical resistivity in pure Fe and Fe-Si alloys with 7–40 at. % Si: each curve is shifted along the ordinate. The arrows indicate the Curie temperatures T_C .

In Fig. 3, the residual resistivity ρ_0 of Fe-Si alloys is plotted against the Si content. The present data (●) are obtained by extrapolation to 0 K in Fig. 2, and the other results have been taken from Schwerer *et al.*¹⁷ (×) and Muir *et al.*¹⁸ (+). The residual resistivity increases with the Si content at first but, above 15 at. % Si, decreases, unlike ordinary solid solutions. Consequently, the value of ρ_0 falls rapidly towards the stoichiometric Fe₃Si with the minimum ρ_0 of 2.3 $\mu\Omega$ cm, which is comparable to that of pure Fe. This demonstrates that Fe₃Si used in the present study is in an almost perfectly ordered state. With a further addition of Si greater than 25 at. %, however, the residual resistivity again increases because of a two-phase (ϵ and DO_3) state.

B. (Fe_{1-x}M_x)₃Si pseudobinary system

Figure 4 shows the temperature dependence of the electrical resistivity in (Fe_{0.8}M_{0.2})₃Si with M=V, Cr, Mn, Co, and Ni.¹⁹ The resistivity curve of Fe₃Si is also represented by the dotted line. The arrows indicate the Curie temperatures T_C . The electrical resistivity for M=V increases rapidly at low temperatures, reaches a maximum near T_C and, above T_C , decreases dramatically with rising temperature. Such an abnormal negative temperature dependence has also been found for M=Cr and Mn,²⁰ and for M=Ti with $x < 0.2$, whereas the resistivity for M=Co and Ni exhibits a temperature dependence similar to that of Fe₃Si. Therefore, the substitution of 3d elements to the left of Fe in the periodic table seems to be liable for the occurrence of the negative temperature dependence of the resistivity. This fact might imply the correlation between the resistance maximum and the Fe_I site selection of these substituting atoms. In other words, the elements with less than half-filled 3d states are more effective for the anomaly than those with more than half-filled ones. Since the substitution of M=Ti, V, Cr, and Mn always causes a sharp reduction in T_C and in magnetization, the anomalous resistance behavior may be attributed to a weakening of ferromagnetism of Fe₃Si compelled by the substituents.

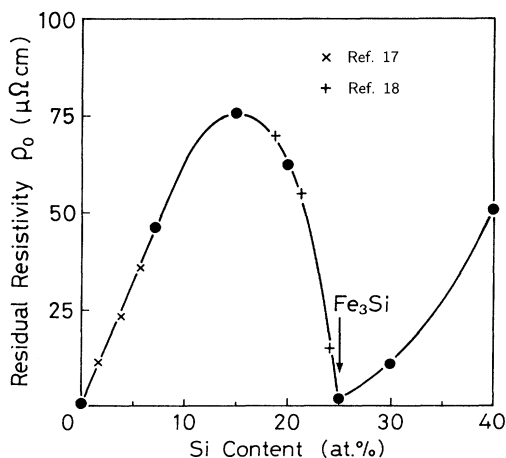


FIG. 3. Residual resistivity ρ_0 as a function of Si content in Fe-Si alloys (●). Also plotted are the data taken from Ref. 17 (×) and Ref. 18 (+).

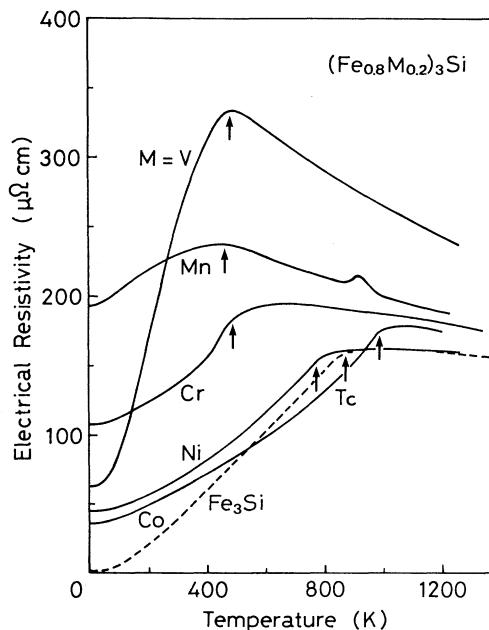


FIG. 4. Temperature dependence of electrical resistivity in (Fe_{0.8}M_{0.2})₃Si with M=V, Cr, Mn, Co, and Ni. The curve of Fe₃Si is also shown by the dotted line. The arrows indicate the Curie temperatures T_C .

tributed to a weakening of ferromagnetism of Fe₃Si compelled by the substituents.

The most spectacular feature of the anomalous resistance behavior has been found for (Fe_{1-x}V_x)₃Si as shown in Fig. 5, as well as for (Fe_{1-x}V_x)₃Ga.¹² It is evident that the tendency of the negative temperature dependence of the resistivity increases markedly with the V composition, in parallel with a reduction in T_C . Thus, the resistance maximum for $x=0.2$ occurs at a relatively low temperature of around 450 K. Because atomic diffusion in this temperature range is too slow for any significant structural change, the negative temperature dependence cannot be explained in terms of an order-disorder transition.

On the other hand, the temperature dependence of the electrical resistivity in (Fe_{1-x}Co_x)₃Si is shown in Fig. 6. It should be remembered that the single-phase state of the DO_3 structure is maintained up to $x=0.6$ for M=Co, as seen in Fig. 1. In contrast with the case for (Fe_{1-x}V_x)₃Si, however, the resistivity curves in Fig. 6 have almost the same form as that of Fe₃Si, without regard to the Co composition. It seems that the resistance maximum near T_C , as in Fig. 5, could hardly be found for M=Co and Ni.

In Fig. 7, the residual resistivity ρ_0 of (Fe_{1-x}V_x)₃Si and (Fe_{1-x}Co_x)₃Si is plotted against composition x . The dependence of ρ_0 on the V or Co composition is not simply linear but parabolic, similar to that of Fe-Si alloys as shown in Fig. 3. The compositions at which ρ_0 reaches a minimum in the respective alloys are estimated to be $x=0.3$ for M=V and $x=0.6$ for M=Co, both of which

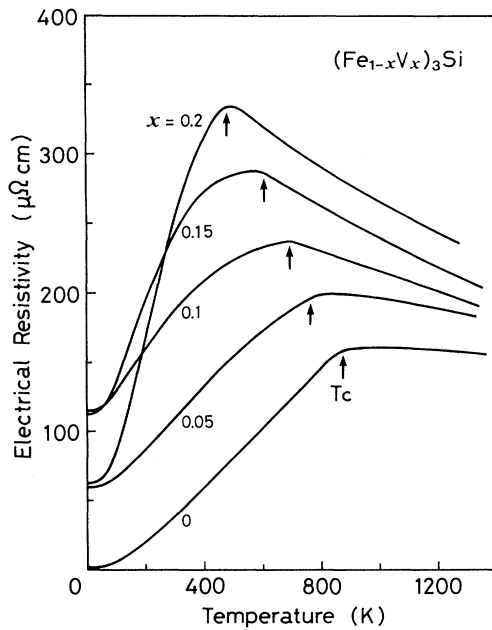


FIG. 5. Temperature dependence of electrical resistivity in $(\text{Fe}_{1-x}\text{V}_x)_3\text{Si}$ with $0 \leq x \leq 0.2$. The arrows indicate the Curie temperatures T_C .

are close to the constitutions of Heusler-type alloys,²¹ Fe_2VSi and FeCo_2Si , respectively. These ordered structures can be formed in $[\text{Fe}_I][\text{Fe}_{II}]_2\text{Si}$ when V atoms selectively occupy the Fe_I site alone or when Co atoms the Fe_{II} site alone. Accordingly, the rapid decrease in the residual resistivity of these alloys is associated with the formation of the Heusler-type ($L2_1$) structure, providing further information on the site preference of the substituting M atoms at high compositions. Another feature to be noted in Fig. 7 is that the value of ρ_0 for $M=\text{V}$ increases first at an extremely large rate of $15 \mu\Omega \text{ cm}$ per

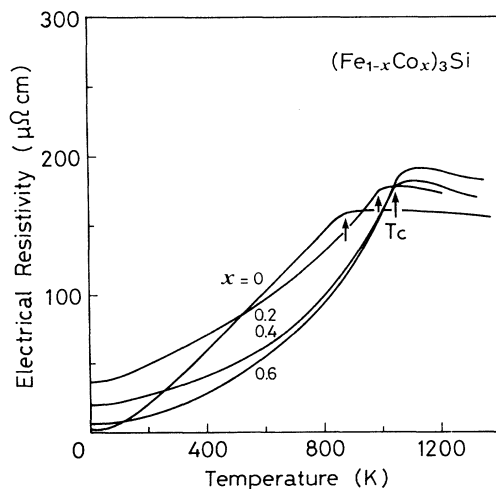


FIG. 6. Temperature dependence of electrical resistivity in $(\text{Fe}_{1-x}\text{Co}_x)_3\text{Si}$ with $0 \leq x \leq 0.6$. The arrows indicate the Curie temperatures T_C .

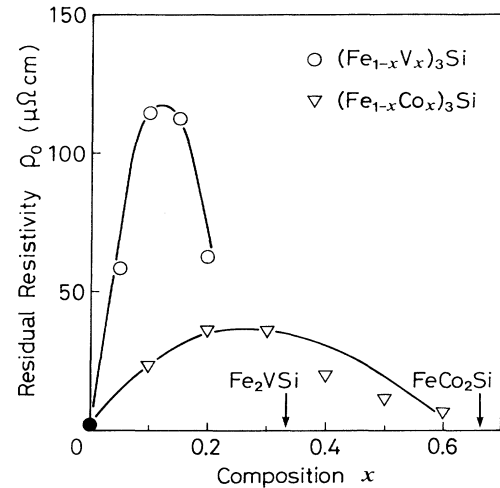


FIG. 7. Residual resistivity ρ_0 as a function of composition x in $(\text{Fe}_{1-x}\text{V}_x)_3\text{Si}$ (\circ) and $(\text{Fe}_{1-x}\text{Co}_x)_3\text{Si}$ (∇). The arrows indicate the compositions to form a Heusler-type structure, Fe_2VSi or FeCo_2Si , respectively.

at. % V and is generally higher, i.e., $60\text{--}120 \mu\Omega \text{ cm}$, than that for $M=\text{Co}$.

IV. DISCUSSION

A. Relation between paramagnetic resistivity and negative resistivity slope

The anomalous temperature dependence of the electrical resistivity observed in $(\text{Fe}_{1-x}\text{M}_x)_3\text{Si}$ can be represented schematically by the upper curve (a) in Fig. 8, as compared with that of an ordinary ferromagnet shown by the lower curve (b). The existence of such a negative resistivity slope shows a breakdown of Matthiessen's rule. In order to consider the anomalous resistance behavior, we suppose the resistivity curve in the paramagnetic state, $\rho_{pm}(T)$, below the Curie temperature T_C , as shown by the dotted lines. The $\rho_{pm}(T)$ curve is obtained by extrapolating the linear part of the resistivity curve observed above T_C . It is now possible to compare the $\rho_{pm}(T)$ term with the temperature slope of the linear part above T_C . Further, the maximum value of the magnetic scattering resistivity, ρ_m^* , can also be evaluated as the difference between $\rho_{pm}(0)$ and ρ_0 , as will be discussed later.

Figure 9 shows the paramagnetic resistivity $\rho_{pm}(T)$, estimated at $T=0, 500$, and 1000 K , plotted against the temperature coefficient of the resistivity, $d\rho/dT$ ($T > T_C$), for $M=\text{V, Cr, Mn, Co, and Ni}$. The value of $\rho_{pm}(T)$ at the respective temperature increases with an increase in the absolute value of $d\rho/dT$. It should be remarked that the variation of $\rho_{pm}(T)$ depends hardly on the substituting M atoms but on the slope $d\rho/dT$ alone. Thus, the $\rho_{pm}(T)$ term can be uniquely expressed as a linear function of $d\rho/dT$ at any temperature. A similar kind of a negative temperature dependence has been found not only in various disordered alloys containing transition metals, as discussed in our paper,¹² but also

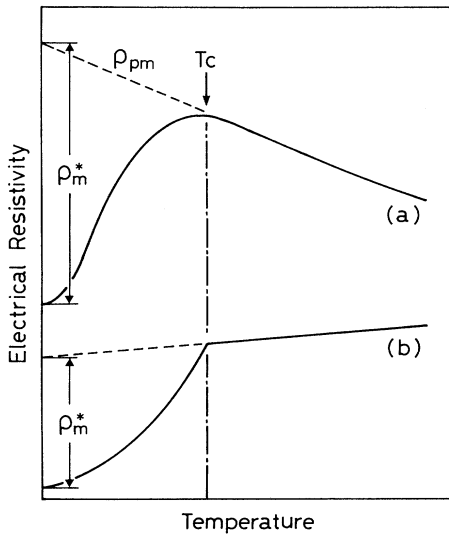


FIG. 8. Schematic illustration of the temperature dependence of electrical resistivity for $(\text{Fe}_{1-x}\text{M}_x)_3\text{Si}$ [curve (a)] and an ordinary ferromagnet [curve (b)]. T_C represents each Curie temperature. The resistivity curves in the paramagnetic state, $\rho_{pm}(T)$, are shown by the dotted lines. The difference between $\rho_{pm}(0)$ and ρ_0 corresponds to the maximum magnetic resistivity ρ_m^* .

in intermetallic compounds such as Al_3Ti alloyed with Mn.²² Mooij²³ has suggested that a high electrical resistance in metallic conductors generally tends to reduce a temperature coefficient of resistivity, finally making it negative above a critical value of resistivity. This might occur regardless of details of the electronic structure of conductors, as noted by Isino and Muto.²⁴ In Fig. 9, all curves seem to converge towards $\rho_{pm}(T)$ around 150

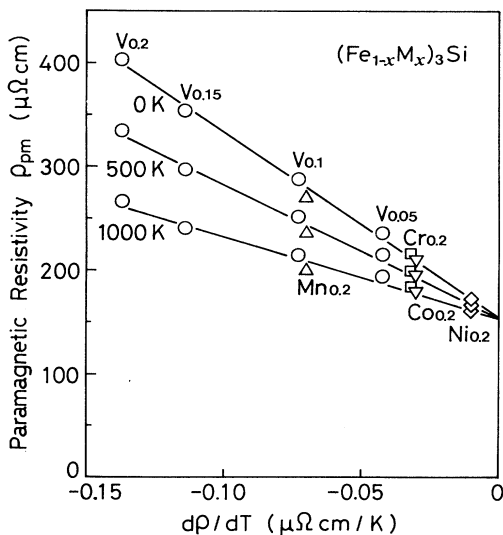


FIG. 9. Paramagnetic resistivity ρ_{pm} , at $T=0, 500$, and 1000 K, as a function of the temperature coefficient of resistivity, $d\rho/dT$, in $(\text{Fe}_{1-x}\text{M}_x)_3\text{Si}$ with $M = \text{V, Cr, Mn, Co, and Ni}$.

$\mu\Omega\text{ cm}$ at $d\rho/dT=0$, and above this critical value of $\rho_{pm}(T)$, its temperature coefficient is always negative for all the alloys, in accordance with Mooij's criterion. In the case of $(\text{Fe}_{1-x}\text{M}_x)_3\text{Si}$, magnetism also plays an important role: the negative temperature dependence appears only above T_C , and loss of magnetic scattering is the main cause for the resistivity change below T_C .

B. Anomaly in magnetic scattering resistivity

The maximum value of the magnetic scattering resistivity, ρ_m^* , is considered to be proportional to the weighted sum of $S(S+1)$, i.e., the quantum-mechanical square of the atomic spin S , as discussed by Weiss and Marotta:²⁵

$$\rho_m^* = \alpha \sum_i p_i S_i(S_i + 1), \quad (1)$$

where a subscript i denotes the Van Vleck configuration²⁶ corresponding to each atomic spin S_i of $3d$ elements, and p_i is its populational probability. It is known that α is almost constant, i.e., $\alpha = 31.2 \pm 1$ for most $3d$ metals and alloys,²⁵ although it comprises various factors such as the s - d interaction energy coefficient G , the conduction electron number per atom, n , and the atomic density N , i.e.,

$$\alpha = (3\pi^2 N)^{1/3} (mG)^2 / 4\pi e^2 n \hbar^3, \quad (2)$$

where m and \hbar are the electron mass and Planck's constant over 2π , respectively, and G is $15.5 \pm 3.5 \text{ eV \AA}^3$ for most $3d$ metals and alloys.²⁵ Proper calculation of $S_i(S_i+1)$ requires the use of half-integer S_i after the Van Vleck model.²⁶ However, we introduce an approximation to use μ_j/g ($g=2$), instead of S_i , where μ_j is the saturation moment of atom j at 0 K and g denotes the Landé g factor. Thus, Eq. (1) can be modified to

$$\rho_m^* = \alpha \sum_j p_j \left[\frac{\mu_j}{g} \right] \left[\frac{\mu_j}{g} + 1 \right], \quad (3)$$

where p_j is taken as a composition of atom j . It has been confirmed in our previous paper¹² that the linear dependence of ρ_m^* on $\sum p_j S_i(S_i+1)$ in Eq. (1) is well reproduced for ordinary $3d$ metals and alloys in terms of Eq. (3) with $\alpha=32$, despite the approximation of μ_j/g .

Figure 10 represents the relation between ρ_m^* and $\sum p_j (\mu_j/g)(\mu_j/g+1)$ for Fe-Si binary alloys, and $(\text{Fe}_{1-x}\text{V}_x)_3\text{Si}$ and $(\text{Fe}_{1-x}\text{Co}_x)_3\text{Si}$ alloys. Here, the moments μ_j were evaluated from the saturation magnetization data of Niculescu *et al.*^{13,27,28} on the simplest assumption that for $(\text{Fe}_{1-x}\text{V}_x)_3\text{Si}$, Fe atoms alone have a magnetic moment to compose the bulk saturation magnetization, and for $(\text{Fe}_{1-x}\text{Co}_x)_3\text{Si}$, both Fe and Co atoms have an equal magnetic moment. The results on pure Fe and Fe-7 at. % Si naturally follow the relation for $\alpha=32$ represented by the dash-dotted line, which can fit most data on ordinary $3d$ metals and alloys. On the formation of the $D0_3$ phase above 15 at. % Si, however, the value of ρ_m^* turns to increase remarkably, as shown by the dotted line, deviating from the linear relation for $\alpha=32$. Thus, Fe_3Si ($x=0$) has a very large ρ_m^* of about $170 \mu\Omega\text{ cm}$, despite an extremely small ρ_0 .

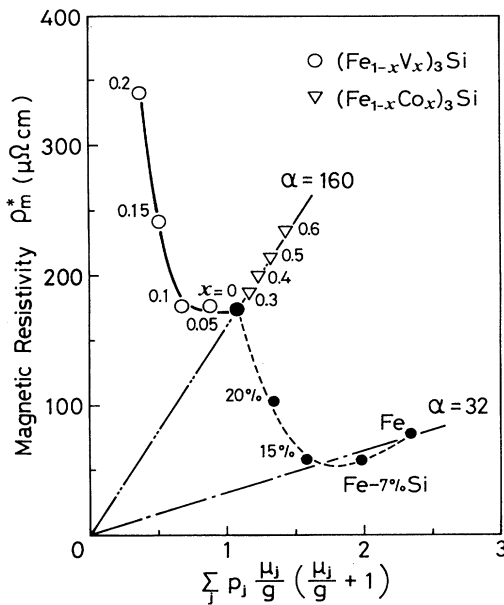


FIG. 10. The maximum value of magnetic resistivity, ρ_m^* , versus $\sum p_j(\mu_j/S)(\mu_j/S+1)$ for Fe-Si (\bullet), $(\text{Fe}_{1-x}\text{V}_x)_3\text{Si}$ (\circ), and $(\text{Fe}_{1-x}\text{Co}_x)_3\text{Si}$ (∇). The relation for $\alpha=32$ (---) fits most data on ordinary 3d ferromagnets in terms of Eq. (3), but the relation for $\alpha=160$ (- - -) is required to fit the data on Fe_3Si and $(\text{Fe}_{1-x}\text{Co}_x)_3\text{Si}$.

Meanwhile, the value of ρ_m^* for $(\text{Fe}_{1-x}\text{Co}_x)_3\text{Si}$ further increases with the Co composition, in parallel with a visible increase in the Fe and Co moments. Consequently, these results show a surprisingly linear variation with the slope of $\alpha=160$, as shown in Fig. 10, which is five times as large as that of ordinary 3d alloys. These results, including that on Fe_3Si , are to be classified as the first case where the resistivity gradually decreases above T_C but its temperature coefficient hardly changes with the Co composition. On the other hand, the value of ρ_m^* for $(\text{Fe}_{1-x}\text{V}_x)_3\text{Si}$ first remains almost constant but, above $x=0.1$, increases dramatically despite a decrease in the Fe moments, deviating from the linear relation for $\alpha=160$. In this second case, the negative temperature dependence tends to increase markedly with the V composition, as observed in Fig. 5: however, this extreme deviation might be ascribed to the intrinsic limitation in the original approximation, $\mu_j/g \approx S_i$, itself.

On the assumption of Eq. (3), there are two possible interpretations for the large α or the above discrepancy in ρ_m^* : "large G " and "small n " in reference to Eq. (2) since the atomic density N of $(\text{Fe}_{1-x}\text{M}_x)_3\text{Si}$ is close to that of Fe and other 3d metals. In the first case, as in Fe_3Si and $(\text{Fe}_{1-x}\text{Co}_x)_3\text{Si}$, the residual resistivity is relatively low, so that the number of n cannot be small as compared with that of Fe and other 3d metals. This means that the linear relation for $\alpha=160$ may be attributed to "large G " alone. The magnitude of G is then estimated to be more than double that of ordinary 3d ferromagnets because G

depends on the square root of α . In contrast, the second case as in $(\text{Fe}_{1-x}\text{V}_x)_3\text{Si}$ can be characterized by an extremely large ρ_m^* , five to twenty times as large as those of ordinary 3d ferromagnets, and yet a very large ρ_0 . This strongly suggests an exceptionally "small n ," in addition to "large G ." A simple explanation for the negative temperature dependence may be possible if it is assumed that conduction electrons increase with rising temperature. For a better understanding of the conduction phenomena in these alloys, magnetoresistance measurements are in progress, which will give more detailed information on the spin disorder scattering. Also, it is desirable to investigate the conduction electron number n by Hall-effect measurements and/or other Fermiological methods, and the true atomic moments by neutron diffraction.

V. CONCLUSIONS

In the $(\text{Fe}_{1-x}\text{M}_x)_3\text{Si}$ system, with $M=\text{Ti}, \text{V}, \text{Cr}, \text{Mn}, \text{Co},$ and Ni , the $D0_3$ phase can always be stabilized much more than in Fe_3Si . The dependence of the residual resistivity on the V or Co composition demonstrates that each resistivity reaches a minimum at the composition of a Heusler-type alloy, Fe_2VSi or FeCo_2Si , respectively. This suggests the selective site substitution at high compositions: V atoms preferentially enter the Fe_I site in the $D0_3$ lattice up to $x=0.3$, while Co atoms occupy the Fe_{II} site up to $x=0.6$.

The electrical resistivity for $M=\text{Ti}, \text{V}, \text{Cr},$ and Mn decreases with rising temperature above the Curie point, which implies an occurrence of a negative temperature coefficient unlike the cases for ordinary 3d metal ferromagnets. However, the resistivity curves for $M=\text{Co}$ and Ni exhibit a similar form to that of Fe_3Si , without regard to the Co or Ni composition. Namely, the 3d elements to the left of Fe in the periodic table are more effective for the anomaly. This suggests the close correlation between the resistance maximum and the Fe_I site selection of the substituents.

The negative temperature dependence induced by M substitution appears only above the critical resistivity of $150 \mu\Omega \text{ cm}$ in the paramagnetic state, in accordance with Mooij's criterion, and the higher paramagnetic resistivity causes the lower, i.e., the more negative temperature coefficient. In contrast to other disordered transition-metal alloys with a negative resistivity slope, $(\text{Fe}_{1-x}\text{M}_x)_3\text{Si}$ has an extremely large magnetic scattering resistivity, in addition to the anomaly in the residual resistivity.

ACKNOWLEDGMENTS

The authors are grateful to K. Kitagawa and S. Tamaoka for their assistance in the electrical resistivity measurements, and to Dr. Y. Saeki for his support in the x-ray measurements. We also wish to thank Professor T. Miyazaki for continuous encouragement throughout this work.

- ¹T. J. Burch, T. Litrenta, and J. I. Budnick, *Phys. Rev. Lett.* **33**, 421 (1974).
- ²S. Pickart, T. Litrenta, T. Burch, and J. I. Budnick, *Phys. Lett. A* **53**, 321 (1975).
- ³C. Blaauw, G. R. MacKay, and W. Leiper, *Solid State Commun.* **18**, 729 (1976).
- ⁴J. I. Budnick, Zhengquan Tan, and D. M. Pease, *Physica B* **158**, 31 (1989).
- ⁵V. A. Niculescu, T. J. Burch, and J. I. Budnick, *J. Magn. Magn. Mater.* **39**, 223 (1983), and references therein.
- ⁶T. J. Burch, J. I. Budnick, V. A. Niculescu, K. Raj, and T. Litrenta, *Phys. Rev. B* **24**, 3866 (1981).
- ⁷A. C. Swintendick, *Solid State Commun.* **19**, 511 (1976).
- ⁸E. J. D. Garba and R. L. Jacobs, *J. Phys. F* **16**, 1485 (1986).
- ⁹J. Kudrnovsky, N. E. Christensen, and O. K. Andersen, *Phys. Rev. B* **43**, 5924 (1991).
- ¹⁰N. Kawamiya and K. Adachi, *J. Magn. Magn. Mater.* **31-34**, 145 (1983).
- ¹¹Y. Nishino, M. Matsuo, S. Asano, and N. Kawamiya, *Scr. Metall. Mater.* **25**, 2291 (1991).
- ¹²N. Kawamiya, Y. Nishino, M. Matsuo, and S. Asano, *Phys. Rev. B* **44**, 12406 (1991).
- ¹³V. Niculescu and J. I. Budnick, *Solid State Commun.* **24**, 631 (1977).
- ¹⁴W. B. Pearson, *A Handbook of Lattice Spacings and Structures of Metals and Alloys* (Pergamon, London, 1958).
- ¹⁵T. Takezawa and T. Yokoyama, *J. Jpn. Inst. Metals* **39**, 550 (1975).
- ¹⁶T. Takezawa, T. Miwa, and T. Yokoyama, *J. Jpn. Inst. Metals* **51**, 285 (1987).
- ¹⁷F. C. Schwerer, J. W. Conroy, and S. Araj, *J. Phys. Chem. Solids* **30**, 1513 (1969).
- ¹⁸W. B. Muir, J. I. Budnick, and K. Raj, *Phys. Rev. B* **25**, 726 (1982).
- ¹⁹The resistivity curves on heating and on cooling almost coincided with each other. All the resistivity data show the curves on heating.
- ²⁰The irregular hump of the resistivity for $M = \text{Mn}$ was observed around 900 K on heating, but upon cooling the hump was rather small or sometimes did not appear at all.
- ²¹V. Niculescu, T. J. Burch, K. Raj, and J. I. Budnick, *J. Magn. Magn. Mater.* **5**, 60 (1977).
- ²²S. R. Nishitani, K. Masaki, Y. Shirai, and M. Yamaguchi, *Scr. Metall. Mater.* **25**, 1921 (1991).
- ²³J. H. Mooij, *Phys. Status Solidi A* **17**, 521 (1973).
- ²⁴M. Isino and Y. Muto, *J. Phys. Soc. Jpn.* **54**, 3839 (1985).
- ²⁵R. J. Weiss and A. S. Marotta, *J. Phys. Chem. Solids* **9**, 302 (1959).
- ²⁶J. H. Van Vleck, *Rev. Mod. Phys.* **25**, 220 (1953).
- ²⁷V. Niculescu, K. Raj, J. I. Budnick, T. J. Burch, W. A. Hines, and A. H. Menotti, *Phys. Rev. B* **14**, 4160 (1976).
- ²⁸V. Niculescu, J. I. Budnick, W. A. Hines, K. Raj, S. Pickart, and S. Skalski, *Phys. Rev. B* **19**, 452 (1979).